

Satellite-Derived Upper Layer Heat Content in Equatorial Atlantic: Comparison with PIRATA buoys

Wilton Zumpichiatti Arruda*

Universidade Federal do Rio de Janeiro (UFRJ) – Instituto de Matemática
Ilha do Fundão, C.P. 68530 - 21945-970 - Rio de Janeiro – RJ, Brasil
wilton@im.ufrj.br

Carlos Alexandre Domingos Lentini*

Universidade Federal da Bahia (UFBA) – Instituto de Física
Travessa Barão de Jeremoabo, s/n, Campus Ondina, Salvador - BA, Brasil
clentini@ufba.br

*Grupo de Oceanografia Tropical – www.goat.fis.ufba.br

Abstract. In this work, the satellite-derived Upper Layer Heat Content (ULH) is estimated for the Equatorial Atlantic. This is achieved combining Sea High Anomalies (SHA) from AVISO, Sea Surface Temperature (SST) from the TRMM Microwave Imager, and climatological subsurface data from the World Ocean Atlas 2001 (WOA01) to a regional reduced gravity model. Maps of ULH are generated from 1992 to 2006. These maps are potentially important to study the heat storage variability in the area of study. In order to validate the satellite-derived ULH data, a comparison between satellite-derived upper layer data and independent *in situ* data from Pilot Research Moored Array in the Atlantic (PIRATA) is performed. Due to the availability of PIRATA data, this comparison is done for the years 1998 to 2006. The results show that the satellite-derived ULH and ULH are highly correlated to their *in situ* counterparts at short to long time scales in general. The seasonal *in situ*- and satellite-derived ULH are also estimated allowing the investigation of the interannual variability of ULH anomalies (ULHA) at the three selected PIRATA mooring sites: (0°N,23°W), (6°S,10°W) and (8°N,38°W). Results of PIRATA buoys which behave similarly to the ones described here are not shown. The ULHA show a tendency for positive warmer anomalies starting from 2003 on, except at the PIRATA buoy located at (6°S,10°W). The results indicate that this satellite-derived methodology is a valuable tool to study climate variability on the Equatorial Atlantic due to its spatial and temporal coverage. We believe that merging the PIRATA data into the WOA01 database could further improve the method.

Keywords: SHA, SST, upper layer, heat content, climate variability, PIRATA, Equatorial Atlantic, anomalies.

Palavras-chave: SHA, TSM, camada superior, conteúdo de calor, variabilidade climática, Atlântico Equatorial, anomalias.

1. Introduction

One of the main goals of climate variability research is the prediction of relatively long-term changes in global climate. Due to the ocean's high thermal inertia, it is believed that the Earth's climate is adjusted by the ocean's troposphere, where heat flux exchange plays a vital role on air-sea process. Therefore, the amount of heat within the upper layer of the ocean is crucial to understanding the coupling between the atmosphere and the ocean, and how they influence each other from short to long time scales.

The lack of continuous long-term hydrographic observations in some regions, especially in the South Atlantic Ocean, makes satellite-derived data an extremely useful tool to investigate time and spatial variability on a basin scale. Altimeter data, which is not affected by cloud coverage as infrared-derived data, provides extremely useful information on the vertical thermal and dynamical structure of the upper ocean when combined with climatological hydrographic through a diagnostic model (Goni et al., 1996; Garzoli and Goni, 2000, Lentini et al. 2006).

Current research and operational global atmosphere and ocean models rely on satellite-based data for forecasting purposes and studies on climate variability. Therefore, the understanding of how the amount of heat stored in the ocean's upper layer varies is crucial. The upper layer heat content can be defined as the amount of heat stored in a layer bounded

below by an isotherm representative of the main thermocline. Assuming the dynamics of the upper layer of the ocean can be reproduced by a reduced gravity model, Arruda et al. (2005) calculated Upper Layer Heat Content (ULH) from climatological ocean data and satellite-based Sea High Anomaly (SHA) and Sea Surface Temperature (SST). The authors used this approach to investigate the physical terms that compose the ULH, its annual cycle, and the variability of its anomalies (hereafter ULHA) on the main dynamical regions in the South Atlantic.

The objective of this work is to compare the ULH with the one calculated directly from Pilot Research Moored Array in the Atlantic (PIRATA). This validation will allow the use of synthetic ULH data to study climate variability on the Equatorial Atlantic with high spatial and temporal resolution.

2. Data and Methods

We assume that the upper ocean dynamics can be reproduced by a regional reduced gravity model. Based on previous observations (Meinen and McPhaden, 2000; Vauclair et al., 2004) we take the 20°C isotherm as a good representative of the Equatorial and Tropical Atlantic thermocline. The SHA and climatological subsurface temperature and salinity data are combined in order to obtain an estimate of the depth of the 20°C isotherm (D_{20})

$$D_{20}(x, y, t) = \overline{D}_{20}(x, y) + \frac{g}{g'(x, y)} \eta'(x, y, t), \quad (1)$$

\overline{D}_{20} is the mean climatological depth of the 20°C isotherm, g is the gravity, g' the mean climatological reduced gravity, and η' is the altimetry-derived SHA. The ULH, which is divided by ρC_p and referenced to 20°C, is computed as

$$ULH(x, y, t) = \int_{D_{20}(x, y, t)}^0 (T(x, y, z, t) - 20) dz = (ULT(x, y, t) - 20)D_{20}(x, y, t), \quad (2)$$

where T is the temperature (°C) and the Upper Layer Temperature (ULT) is the mean temperature in the layer between the ocean surface and bounded below by the 20°C isotherm.

Maps of SHA from multimission altimeter data set, distributed by AVISO (Archiving Validation and Interpretation of Satellite Data in Oceanography), are used to retrieve the η' values. The AVISO SHA resolution is $1/3^\circ \times 1/3^\circ$ on a Mercator grid with a spatial resolution of seven days and spanning from 1992 to 2006. We also use the Optimally Interpolated Sea Surface Temperature data (OISST) from the TRMM Microwave Imager (TMI), carried on NASA's Tropical Rainfall Measuring Mission (TRMM) satellite. TMI resolution is $1/4^\circ \times 1/4^\circ$ from 1998 to 2006 with daily files. The climatological temperature and salinity data are derived from the high resolution ($1/4^\circ \times 1/4^\circ$) World Ocean Atlas 2001 (WOA01) (Boyer et al., 2005).

Since subsurface temperature measurements with high space and time coverage are not available, the ULT in (2) is calculated by the following equation

$$ULT(x, y, t) = \alpha_1(x, y)SST(x, y, t) + \alpha_0(x, y), \quad (3)$$

where α_0 and α_1 are the regression coefficients obtained by a linear regression fit to all climatological SST and ULT values from WOA01 in a $4^\circ \times 4^\circ$ box centered at (x, y) . $SST(x, y, t)$ is the sea surface temperature measured by the TMI sensor. In this way, the ULH is calculated according to the expression

$$ULH(x, y, t) = (\alpha_1(x, y)SST(x, y, t) + \alpha_0(x, y) - 20)D_{20}(x, y, t). \quad (4)$$

Using (4) maps of ULH with the same spatial and temporal resolution of the altimetry data from 1992 to 2006 are generated. In order to assure the reliability of this dataset for climatic studies, we perform a comparison with *in situ* data obtained from the Pilot Research Moored Array in the Tropical Atlantic (PIRATA). The buoy locations are selected according to the availability of data covering wider periods of time and with minimum gaps of missing values. The chosen locations are displayed on **Fig.1** (dashed circles). Due to space limitation, we will show the results of only one equatorial buoy at ($0^{\circ}\text{N},23^{\circ}\text{W}$) (since the results for ($0^{\circ}\text{N},35^{\circ}\text{W}$) are similar), only one South Atlantic buoy ($6^{\circ}\text{S},10^{\circ}\text{W}$) (since the results for ($10^{\circ}\text{S},10^{\circ}\text{W}$) are similar), and one North Atlantic buoy ($8^{\circ}\text{N},38^{\circ}\text{W}$).

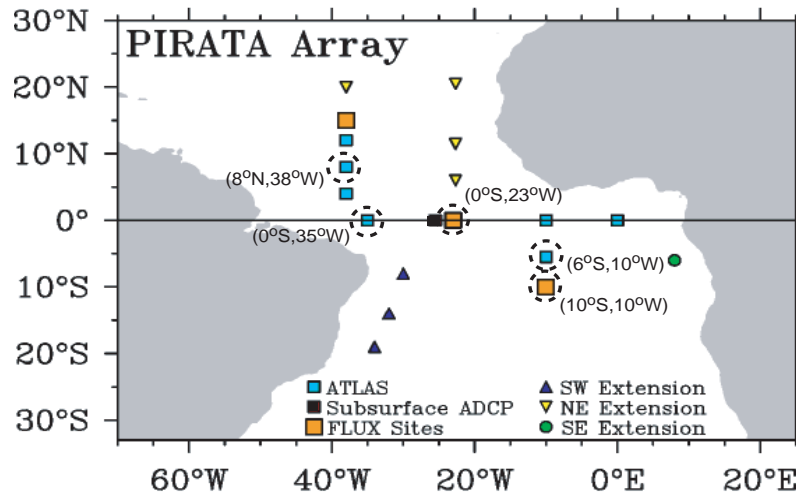


Figure 1. PIRATA array map. The dotted circles indicate the buoy locations where the comparison with the satellite-derived ULH is performed.

3. Discussion

Figures 2-4 show the comparison between the satellite-derived (thick line) D_{20} (upper panels) and ULT (lower panels), to the PIRATA *in situ* data (thin line).

The equatorial buoy ($0^{\circ}\text{N},23^{\circ}\text{W}$) shows an excellent agreement between the estimated D_{20} and ULT and the observed ones.

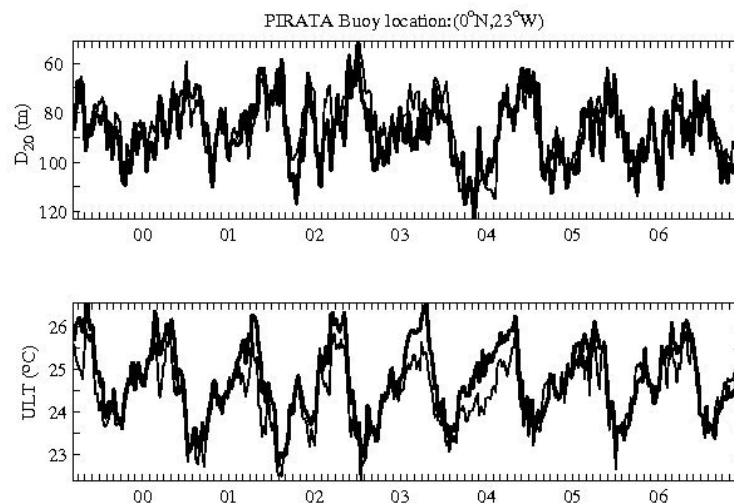


Figure 2. PIRATA buoy location at ($0^{\circ}\text{N},23^{\circ}\text{W}$). Comparison between the depth of the 20°C isotherm, D_{20} , estimated from (1) (thick line) and the depth of the 20°C isotherm derived from the *in situ* PIRATA data (thin line), (upper panel). Same as the D_{20} comparison, except this is for the ULT comparison (lower panel).

At the ($6^{\circ}\text{S}, 10^{\circ}\text{W}$) location, the satellite-derived D_{20} is deeper than the observed D_{20} on the first half of each year from 1994 to 2004. From 2004 on, the satellite-derived D_{20} is shallower than the observed for the remaining years all year-round. At the same location, the estimated ULT is higher than the observed one during summer months.

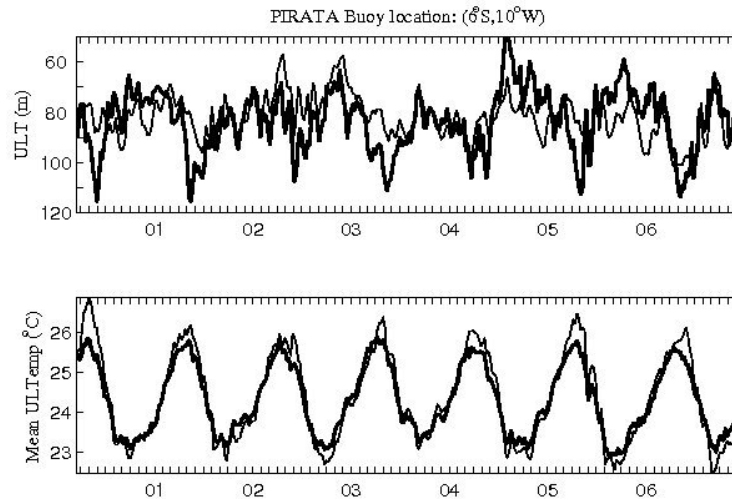


Figure 3. Same as Fig. 2 for PIRATA buoy at ($6^{\circ}\text{S}, 10^{\circ}\text{W}$).

At the northern hemisphere buoy ($8^{\circ}\text{N}, 38^{\circ}\text{W}$), the satellite derived D_{20} matches very well to the observations, except for the second half of the year between 2001 and 2004. Moreover, the estimated ULT is higher than the observed during summer months.

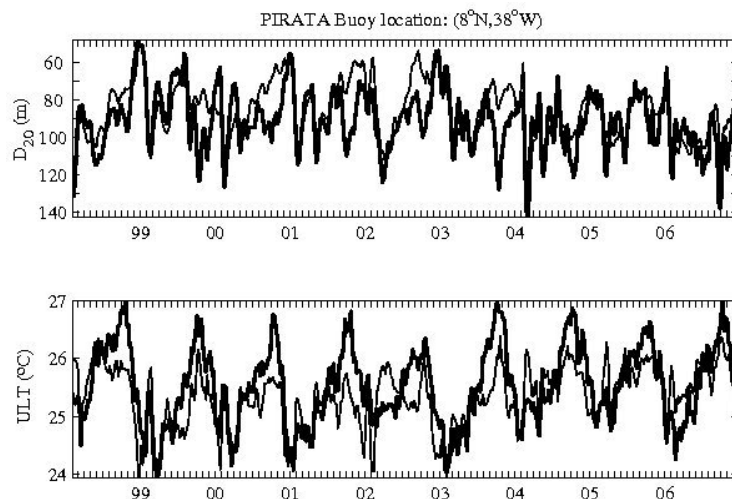


Figure 4. Same as Fig. 2 for PIRATA buoy at ($8^{\circ}\text{N}, 38^{\circ}\text{W}$).

In order to find the reason why remote sensing estimated and in situ ULT differ, we will look carefully into the linear regression fit used in (3). **Fig. 6** displays the scatter plots of SST and ULT from the PIRATA data at the three moored buoys: (a) ($0^{\circ}\text{N}, 23^{\circ}\text{W}$), (b) ($6^{\circ}\text{S}, 10^{\circ}\text{W}$), and (c) ($8^{\circ}\text{N}, 38^{\circ}\text{W}$). On each plot, the linear regression fitted lines between SST and ULT from PIRATA data (red line) and from WOA01 (blue line) data in a $4^{\circ} \times 4^{\circ}$ box centered at each buoy location is also added.

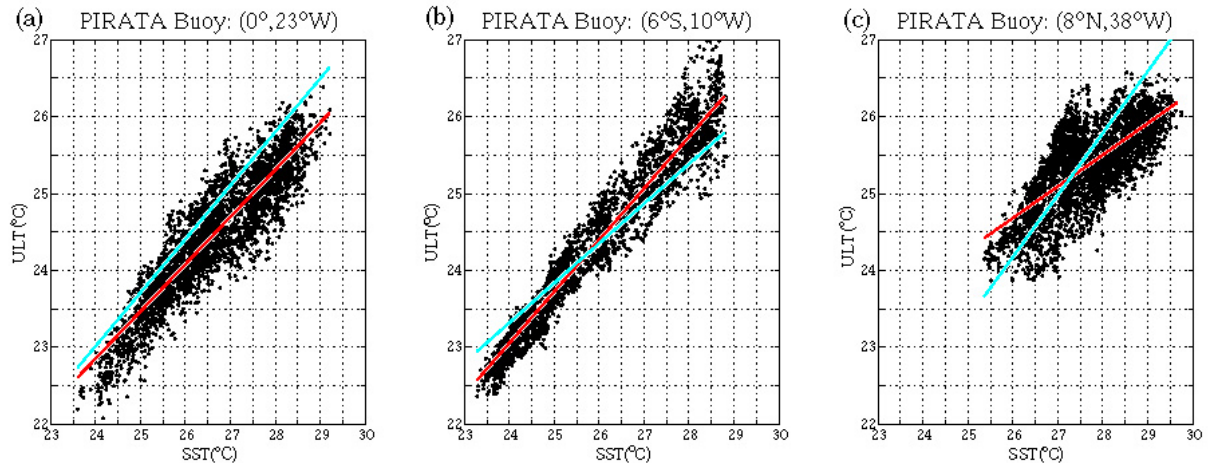


Figure 6. Scatter plot of SST against the mean upper layer averaged temperature from the PIRATA at the three following locations: (a) (0°N,23°W); (b) (6°S,10°W); (c) (8°S,38°W). Solid lines are the linear regression fitted lines calculated for the PIRATA (red line) data at these three locations and for the WOA01 (blue line) data in 4°×4° boxes centered at each PIRATA buoy location.

At the (0°N,23°W) site (**Fig. 6a**), there is a very good linear relationship between SST and ULT ($r^2 = 0.87$). Note that the slope of the regression fit derived from the WOA01 (blue line) data is bigger than the one derived from PIRATA (red line) data at this location. This means that (3) will always overestimate ULT with a larger error for higher SSTs, which causes the observed higher values for estimated ULT during summer months (**Fig. 2**).

At the (6°S,10°W) site (**Fig. 6b**), there is a higher linear relationship between SST and ULT ($r^2 = 0.97$). By using the linear regression coefficients derived from WOA01 climatology (blue line) in (4) the ULT tends to be underestimated in summer with a smaller overestimation in winter (**Fig. 3**).

At the (8°N,38°W) site (**Fig. 6c**), the regression between SST and ULH is only $r^2 = 0.7$. Since the data is more scattered at this site, the estimated ULT from (3) tends to be significantly overestimated in summer and underestimated in winter (**Fig. 4**).

Figs. 7(a)-9(a) show the ULH estimated from (4) (solid line) and its respective seasonal (annual plus semi-annual) cycle (dashed line).

Figs. 7(b)-9(b) show the *in situ*-derived ULH at each buoy location (solid line) and its respective seasonal (annual plus semi-annual) cycle (dashed line). At the (0°N,23°W) site, the satellite-derived ULH amplitude and its respective annual cycle match the *in situ*-derived ULH. On the other hand, the amplitude of the satellite-derived ULH is slightly higher than its *in situ* counterpart at the (6°S,10°W) position. This is probably due to the accumulated errors in the calculation of D_{20} and ULT at this location. At the (8°N,38°W) buoy, there is not a big difference in the amplitude, although there is a marked semi-annual component at the satellite-derived ULH.

Figs. 7(c)-9(c) show the Upper Layer Heat content Anomalies (ULHA), that is, the difference between the ULH and its seasonal cycle for satellite-derived (thick line) and *in situ* (thin line) estimates. It is remarkable that although at the (6°S,10°W) buoy there is a difference between the observed and *in situ* ULH amplitude of the seasonal cycle, the ULHA fall into the same amplitude range and show a very close variability pattern. The filtered ULHA for satellite-derived (thick line) and *in situ* (thin line) estimates are shown on **Figs. 7(d)-9(d)**.

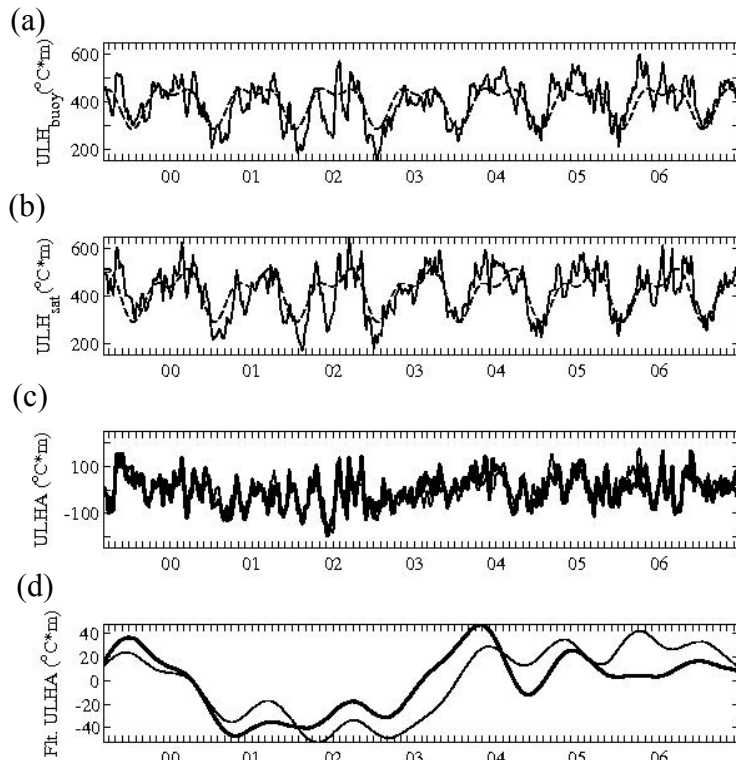


Figure 7. Panels (a-d) are for the PIRATA buoy location at $(0^{\circ}\text{N}, 23^{\circ}\text{W})$. (a) the *in situ*-derived ULHC (solid line) estimated from (4) and its seasonal cycle (dashed line); (b) the satellite-derived ULHC (solid line) calculated at this PIRATA buoy site and its seasonal cycle (dashed line); (c) comparison between the *in situ*-derived ULHA (thick line), which is defined as the difference between ULH and its seasonal cycle in (a), and the satellite-derived ULHA (thin line), which is defined as the difference between ULH and its annual cycle in (b); (d) Same as (c) but low-pass filtered with a cut off frequency of 12 months.

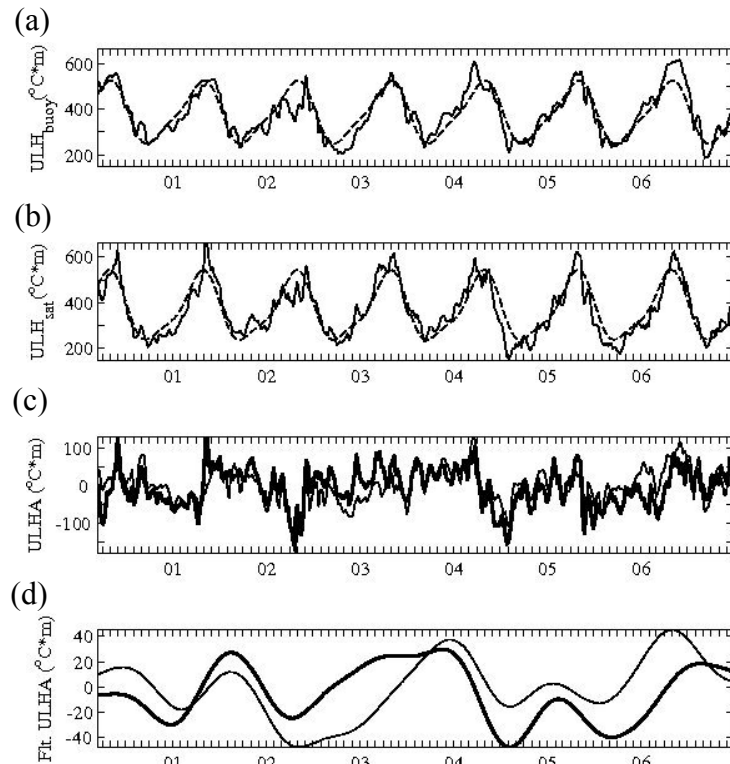


Figure 8. Same as Fig. 7, except this is for the PIRATA buoy site at $(6^{\circ}\text{S}, 10^{\circ}\text{W})$.

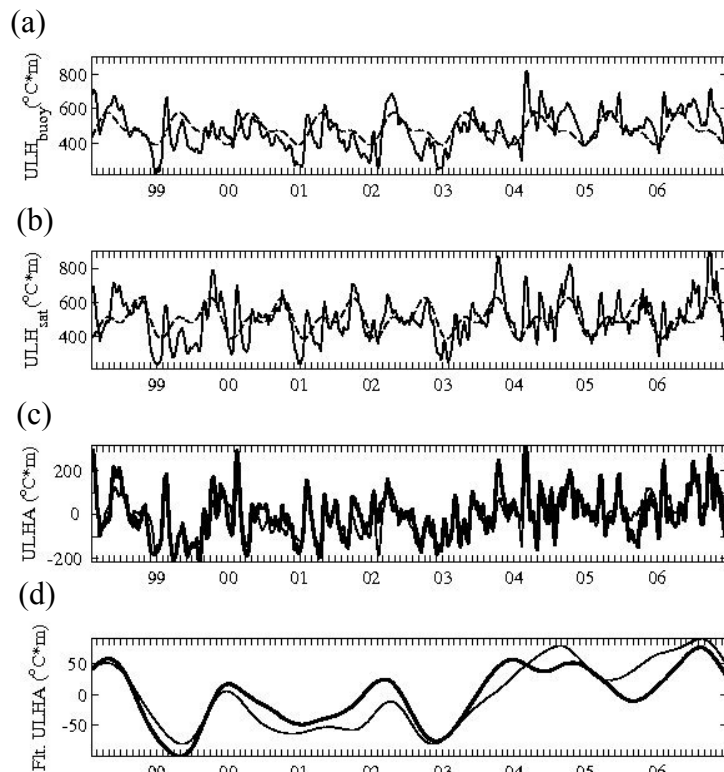


Figure 9. Same as Fig.7, except this is for the PIRATA buoy site at 8°N,38°W.

Comparison among the filtered ULHA (**Figs. 7d, 8d and 9d**) indicate an upward trend starting since mid 1999 (Fig. 9d) and the end of 2000 (Fig. 7d) with a tendency for positive warmer ULHA from 2003 on, except at the PIRATA buoy located at (6°S,10°W) in which the positive trend stars at middle 2004.

4. Conclusions

In this paper compare the Upper Layer Heat Content data derived from remote sensing with *in situ* data collected at three buoys of the PIRATA project. We show that although at the off-equatorial locations there is an error of the predicted ULH annual cycle the anomalies are highly correlated with the its *in situ* counterpart at long time scales. We observe that the ULH annual cycle discrepancies came from the use of WOA01 to estimate the regression coefficients in equations (3) and (4), which makes us believe that merging the PIRATA data at the WOA01 database could further improve the method.

Considering all the approximations implicitly described in equations (1), (3), and (4), we conclude that the derived ULHA fields are a valuable tool to study climate variability on the Equatorial Atlantic due to its spatial and temporal coverage of remote sensing data.

Acknowledgements

The altimeter products were produced by SSALTO/DUACS and distributed by AVISO (www.aviso.oceanobs.com), with support from CNES. Microwave OISST data are produced by Remote Sensing Systems and sponsored by National Oceanographic Partnership Program (NOPP), the NASA Earth Science Physical Oceanography Program, and the NASA REASoN DISCOVER Project. Data are available at www.remss.com. The authors also would like to thank the Brazilian Research and Technology Council (CNPq) for funding the BACANA and VARICONF Projects, grants #478398/2006-9 and #476472/2006-7, respectively.

5. References

Arruda,W.Z.; Lentini, C.A.D.; Campos, E.J.D. The use of satellite derived upper layer heat content to study the climate variability in the South Atlantic. **Brazilian Journal of Cartography**, v. 57, n. 2, 87-92. 2005.

Boyer, T; Levitus, S.; Garcia, H.; Locarnini, R.A.; Stephens, C; Antonov, J. Objective analyzes of annual, seasonal, and monthly temperature and salinity for the world ocean on a 0.25 degrees grid. **International Journal of Climatology**, v. 25, n. 7, 931-945. 2005.

Garzoli, S; Goni, G. Combining altimeter observations and oceanographic data for ocean circulation and climate studies. In: Halpern, D. (Org.). **Satellites Oceanography and Society**, Elsevier Oceanographyc Series, n. 63, 79-95.2000.

Goni, G.; Kamholz, S.; Garzoli, S.; Olson, D.B. Dynamics of the Brazil- Malvinas Confluence based on inverted echosounders and altimetry. **Journal of Geophysical Research**, v. 101, n. C7, 16273-16289. 1996.

Lentini, C.A.D.; G. J. Goni; Olson, D.B. Investigation of Brazil Current Rings: 1993-1998. **Journal of Geophysical Research**, 111, C06013, doi: 10.1029/2005JC002988. 2006

Meinen, C.; McPhaden, M.C. Observations of warm water volume changes in the Equatorial Pacific and their relation to El Niño and La Niña. **Journal of Climate**, v. 13, 3551-3559. 2000.

Vauclair, F.; du Penhoat, Y. Heat and mass budgets of warm upper layer of the Tropical Atlantic Ocean in 1979-99. **Journal of Physical Oceanography**, v.34, n. 4, 904-914. 2004.